Computers and Chemical Engineering xxx (2016) xxx–xxx

Contents lists available at ScienceDirect

Computers and Chemical Engineering

journal homepage: www.elsevier.com/locate/compchemeng

Optimal match between heat source and absorption refrigeration

Yufei Wang[a], Chensheng Wang[a], Xiao Feng[b,*]

[a] State Key Laboratory of Heavy Oil Processing, China University of Petroleum, Beijing 102249, China
[b] School of Chemical Engineering & Technology, Xi'an Jiaotong University, Xi'an 710049, China

ARTICLE INFO

Article history:
Received 5 July 2016
Received in revised form 5 November 2016
Accepted 5 November 2016
Available online xxx

Keywords:
Absorption refrigeration
Coefficient of performance
Exergy efficiency
Temperature of heat source
Refrigeration level

ABSTRACT

In process industries, there is usually a great amount of waste heat available at different temperatures, and at the same time, there are cooling or refrigeration demands at different temperatures. In this paper, a single effect water–lithium bromide absorption refrigeration system is modeled and simulated using the process modeling software Aspen Plus. The optimal matches between heat source temperatures and refrigeration levels of the absorption refrigeration cycle are determined. The performance of the absorption refrigeration cycle is assessed in terms of two indicators: coefficient of performance (COP) and exergy efficiency. At a certain evaporator temperature of the absorption refrigeration cycle, which indicates a certain refrigeration level, the COP of the cycle rises rapidly at first and then gently with increasing heat source temperature because higher temperature generates more refrigerant vapor. The exergy efficiency of the cycle, by contrast, exhibits a maximum value because both the system performance and the system irreversibility increase with increasing heat source temperature. Ensuring a proper match between heat source and absorption refrigeration can lead to efficient use of waste heat and decrease degradation loss of waste heat.

1. Introduction

Most industrial enterprises burn fuel to supply heat, steam and power required by a multitude of processes. These processes typically discharge a great amount of waste heat at different temperatures to the environment. Obviously, considerable energy can be recovered from such waste heat sources. In China, the amount of waste heat discharged by industrial processes accounts for about 17–67% of the consumed fuel, and about 60% of which can be recovered (Lian et al., 2011). In the UK, up to 14 TWh per annum (4% of total energy use) of the process industries' energy consumption is lost as recoverable waste heat (Law et al., 2016). Recovering this type of waste heat can effectively reduce fossil fuel energy consumption, which has a significant and positive relationship with carbon dioxide emissions (Khan et al., 2016). For example, substantial recovery of 14 TWh per annum in the UK would have environmental benefits of hundreds of thousands of tonnes of carbon dioxide equivalent per year (Law et al., 2016).

A number of methods are available for waste heat recovery including direct heat transfer from source-to-sink using heat exchangers (Hammond and Norman, 2014; Law et al., 2016); upgrading waste heat to a more desirable temperature using heat pumps (Hammond and Norman, 2014; Law et al., 2016); conversion of waste heat energy to fulfill a chilling demand using absorption refrigeration (Hammond and Norman, 2014); and conversion of waste heat energy to electrical energy using (Organic) Rankine, or Kalina cycles (Hammond and Norman, 2014; Law et al., 2016; Markides, 2013). Of these options, direct heat transfer is preferred if suitable heat sinks are available (Hammond and Norman, 2014; Markides, 2013). In the absence of suitable heat sinks, when the temperature of the waste heat is in the range of 100–300 °C and the magnitude of the waste heat is less than 3 MWth, absorption refrigeration is the most effective way to recover the waste heat (Hammond and Norman, 2014).

Absorption refrigeration is a cycle that uses waste heat to provide cooling or refrigeration. It uses a refrigerant-absorbent pair as a working fluid, the most common of which are water/lithium bromide (LiBr) and ammonia/water. A basic absorption refrigeration cycle consists of a generator, a condenser, two throttle valves, a pump, an evaporator and an absorber, as shown in Fig. 1. Heat is added at the generator, separating gaseous refrigerant and liquid solution. The gaseous refrigerant is sent to the condenser, where it rejects heat and becomes saturated liquid. It is expanded through throttle valves and then evaporated in the evaporator by receiving heat from a low temperature heat source, resulting in useful cooling/refrigeration. The liquid solution from the generator is also

* Corresponding author.
E-mail address: xfeng@xjtu.edu.cn (X. Feng).

http://dx.doi.org/10.1016/j.compchemeng.2016.11.003
0098-1354/

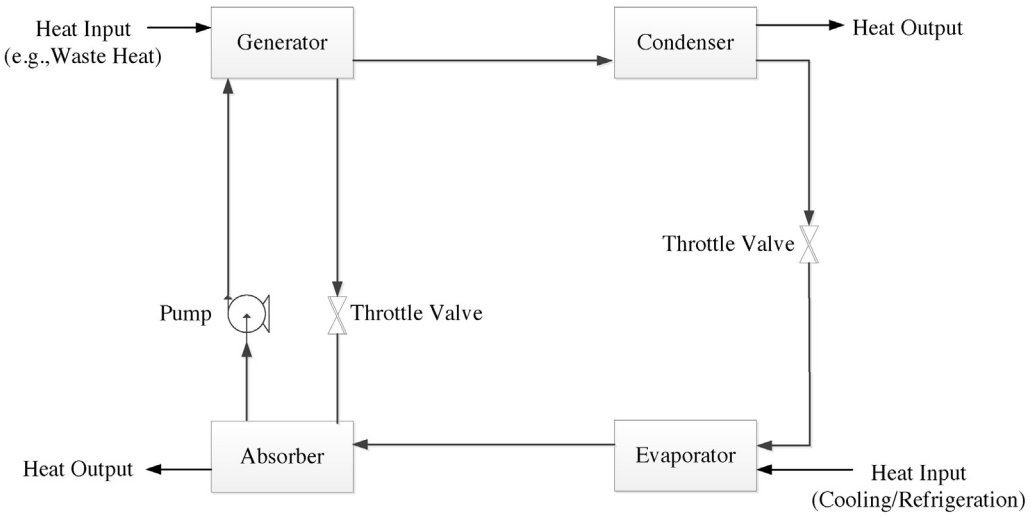

Fig. 1. Schematic diagram of a basic absorption refrigeration cycle.

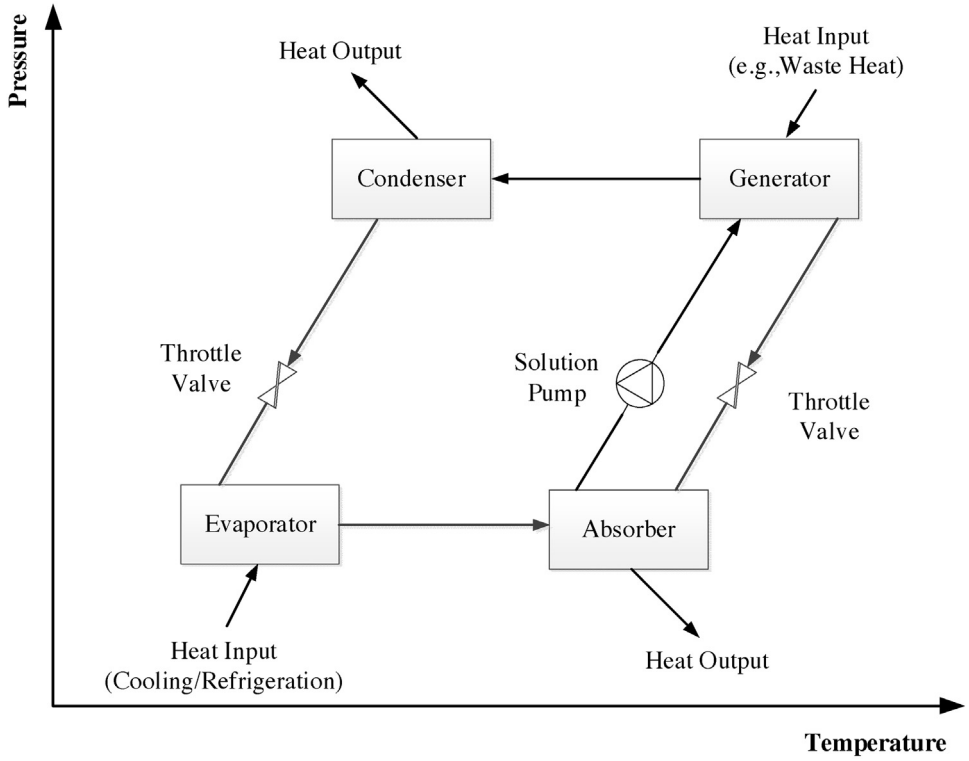

Fig. 2. Temperature-Pressure diagram of a basic absorption refrigeration cycle.

expanded through a throttle valve, and then recombines with the gaseous refrigerant from the evaporator in the absorber through a pump. The corresponding Temperature-Pressure diagram is shown in Fig. 2.

Many studies have been carried out to assess the performance of an absorption refrigeration cycle, mainly based on the coefficient of performance (COP) (Mazzei et al., 2014) or/and exergy efficiency (Gong and Boulama, 2014). Mazzei et al. (2014) established an NLP model to optimize the cycle with COP and the total heat transfer area as the objective function. In this paper, we also use the COP and exergy efficiency indicators to study the energy performance of an absorption refrigeration cycle used to recover waste heat. Karamangil et al. (2010) found that adding a solution heat exchanger to the basic cycle can increase the COP by up to about 66%. This enhancement is due to a reduction in the heat input to the generator. Anand et al. (2013) obtained results similar to those of Karamangil et al. (2010) through simulation for a range of operation temperatures and heat transfer efficiencies obtained with different working fluids. Kaynakli and Kilic (2007) studied the effect of various operation parameters on the COP indicator, and also found that adding a solution heat exchanger can increase the COP by up to about 44%. This paper will also study the basic cycle equipped with a solution heat exchanger.

Some studies investigated the effect of cycle parameters on the system performance. Karamangil et al. (2010) developed a visualized software to simulate the cycle performance and found that the operation temperatures in the generator, absorber, evaporator and condenser affect the cycle performance. COP of the cycle

Please cite this article in press as: Wang, Y., et al., Optimal match between heat source and absorption refrigeration. Computers and Chemical Engineering (2016), http://dx.doi.org/10.1016/j.compchemeng.2016.11.003

increases with increasing operation temperature in the generator and evaporator but decreases with increasing absorber and condenser temperature (Karamangil et al., 2010). Kilic and Kaynakli (2007) adopted the COP and exergy efficiency indicators to evaluate the effect of each component's temperature on the system performance. They also found that COP of the cycle increases with increasing generator and evaporator temperature. Different from the above studies, Fernández-Seara and Vázquez (2001) and Ebrahimi et al. (2015) found that there is an optimal generator temperature. However, COP of the cycle increases first with the generator temperature, and after the temperature reaches the optimal value, COP changes very gently. Therefore, COP almost monotonously changes with all the cycle temperatures. Accordingly, in this paper, we will choose proper cycle temperatures.

Absorption refrigeration cycles with different working fluids have different demands for heat source, and can satisfy cooling or refrigeration requirement at different temperatures. Therefore, it is important to properly match heat source and the refrigeration cycle. In 1985, Reay (1985) proposed three rules for such match: (1) the recovered heat can generate cooling or refrigeration at the required temperature; (2) the recovered heat can economically be transferred from heat source to heat sink; and (3) heat supply and demand should occur at the same time, for heat storage is expensive. Deng et al. (2011) proposed suitable refrigeration cycle that corresponds to a specific heat source temperature. Srikhirin et al. (2001) reviewed appropriate cycles for different working fluids. For three kinds of heat sources, hot water, air and steam, Kaynakli et al. (2015) compared COP and exergy loss for the absorption refrigeration system and found that the biggest exergy loss occurs when air is the heat source while hot water gives the smallest loss. Accordingly, hot water is adopted as the heat source in this paper. Gong and Boulama (2014) used avoidable and inevitable exergy loss to analyze the exergy loss of each component in the cycle. When the temperature of the heat source changes, it is possible to find a point that corresponds to the maximum exergy efficiency, which indicates the optimal match between heat source and the refrigeration demand (Gong and Boulama, 2014). However, no comprehensive analysis is made for finding the optimal match between heat source and the refrigeration demand.

In process industries, there is usually a great amount of waste heat available at different temperatures, and at the same time, there are cooling or refrigeration demands at different temperatures. Determination of the optimal match between the heat source and the cooling or refrigeration demand of an absorption refrigeration cycle can lead to efficient utilization of waste heat and reduction in degradation loss of waste heat. In this paper, a single effect water–lithium bromide absorption refrigeration system that makes use of low temperature waste heat is modeled using the process modeling software Aspen Plus. The optimal matches between heat source temperatures and refrigeration levels of the absorption refrigeration cycle are determined and analyzed.

2. Model of the absorption refrigeration cycle

In a LiBr-H_2O absorption refrigeration cycle, LiBr is the absorbent while H_2O is the refrigerant. The cycle considered in this paper is shown in Fig. 3. Heat is added at the generator, separating gaseous refrigerant and liquid solution. The gaseous refrigerant (steam) is sent to the condenser, where it rejects heat and becomes saturated water. It is expanded through throttle valve RefV and then evaporated in the evaporator by receiving heat from a low temperature heat source, resulting in useful cooling/refrigeration. The liquid solution from the generator is also expanded through throttle valve SolV, and then recombines with the steam from the evaporator in the absorber through a pump. A solution heat exchanger (SHE) is included to improve performance. The hot side of the SHE is placed between the liquid exit of the generator and the solution expansion valve. The cold side is placed between the exit of the pump and the entrance to the generator.

To calculate the physical properties of each state point, which depend on operation conditions and the fluids, a suitable property method should be chosen. The ELECNRTL property method in Aspen Plus is chosen for LiBr-H_2O solution which is an electrolyte solution. The ELECNRTL property method is fully consistent with the NRTL-RK property method, and the molecular interactions are calculated in exactly the same way, therefore ELECNRTL can use the databank for binary molecular interaction parameters in the NRTL-RK property method. To use ELECNRTL properly, the relevant components (in this case, water and lithium bromide) must be selected, and the electrolyte wizard is used, which will generate a series of reactions. In this study, the only relevant reaction is the association/dissociation of lithium bromide (Somers, 2009). In the ELECNRTL property method, enthalpy and entropy are calculated by HLMXELC1 (enthalpy of liquid mixture), HVMX90 (enthalpy of gaseous mixture), SLMXELC1 (entropy of liquid mixture), and SVMX90 (entropy of gaseous mixture), respectively. For the states that are pure water, the steamNBS property method is used, which is based on the International Association of Properties of Steam as

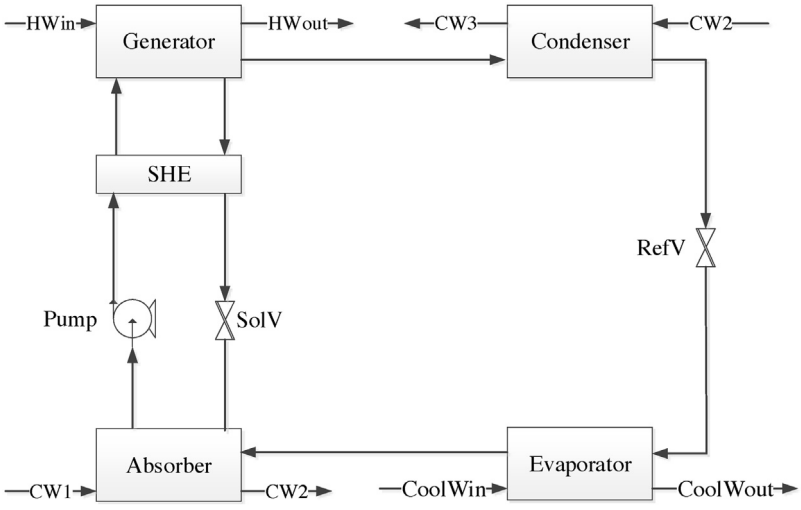

Fig. 3. Schematic diagram of single-effect LiBr-H_2O absorption refrigeration cycle.

Please cite this article in press as: Wang, Y., et al., Optimal match between heat source and absorption refrigeration. Computers and Chemical Engineering (2016), http://dx.doi.org/10.1016/j.compchemeng.2016.11.003

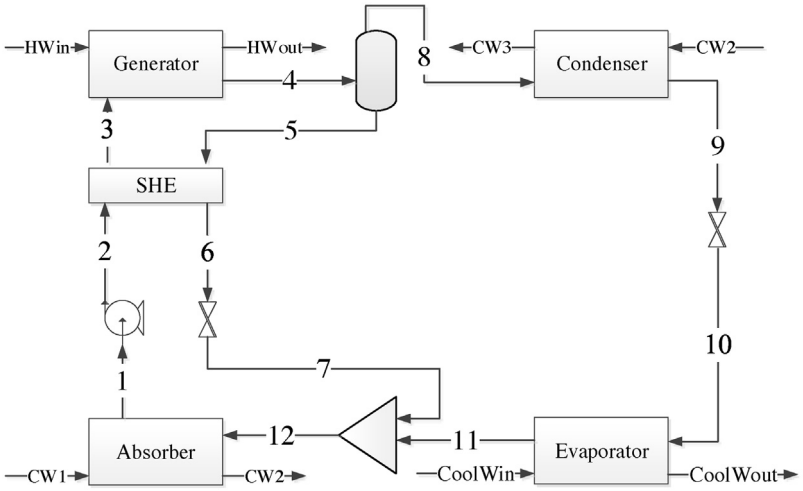

Fig. 4. Simulation model and state points.

Table 1
System state points and assumptions.

State point	Assumption
1	Saturated liquid
2	Determined by the solution pump
3	Determined by the SHE
4	Determined by the heat source
5	Saturated liquid
6	Determined by the SHE
7	Determined by the SolV
8	Saturated vapor under phase equilibrium with state 5
9	Saturated liquid
10	Determined by the RefV
11	Saturated vapor

given in the NBS steam table. The simulation model is illustrated in Fig. 4, and the assumption for each state point in Fig. 4 is given in Table 1.

Modeling the cycle in Aspen Plus is based on modeling each simple component (known as "block") and then connecting them. Many basic components (pumps, valves, etc) can be modeled simply by selecting the equivalent block in Aspen Plus. The components that do not have exact analogues may require further assumptions or multiple blocks to model. Table 2 gives the model for each component and the calculated parameters in each block. The underlying mathematical models that these blocks use are simply mass and energy balances.

Because Aspen Plus uses a sequential solver, given that the absorption refrigeration cycle is a closed cycle, it is necessary to break the cycle to give inputs to the model. In this study, the break is inserted at state point 1 (Fig. 4). In other words, the exit of the absorber (stream 1A) and the inlet of the pump (stream 1) are not connected. Stream 1 is given an initial value. If these two fluid streams have the same results, the model converges. If they are different, the initial value of stream 1 needs to be adjusted.

The cycle model requires only the following inputs: (1) the supply temperature of the heat source; (2) either quantity of heat available or desired cooling load; (3) evaporator exit temperature (related to desired cooling temperature); (4) the supply temperature of cooling water; and (5) the heat transfer efficiency of SHE.

In this paper, the heat source is hot water with flowrate 24 kg/s. This value of the flowrate is taken from an industrial application. Although a flowrate must be specified in the calculation, it should be noted that it does not matter what flowrate value is used because the absorption refrigeration cycle performance is assessed in terms of COP and exergy efficiency which are relative indicators. The supply temperature of the heat source will be varied in this study. Its outlet temperature is the outlet temperature of the solution from the generator plus 10 °C (Kaynakli et al., 2015). This is to guarantee a feasible heat transfer driving force. The concentration of the solution is taken as 0.58 (Kaynakli et al., 2015; Mazzei et al., 2014). The temperature of the condenser is set as 45 °C (Dai, 2001). The heat transfer efficiency of SHE is taken as 0.614 (Gong and Boulama, 2014; Kaynakli et al., 2015; Somers, 2009). The supply temperature of cooling water is set as 25 °C (Kaynakli et al., 2015), which is a typical value.

To evaluate the performance of the cycle, the coefficient of performance (COP) and exergy efficiency indicators will be used.

Table 2
Simulation model of each component.

Component	Block	Calculated parameters
Pump	Pump	Power requirement, temperature, enthalpy and entropy of State 2 are calculated.
SolV	Valve	Temperature and entropy of State 7 are calculated.
RefV	Valve	Temperature and entropy of State 10 are calculated.
SHE	Heater+ Heater	Temperature of State 6, heat duty of SHE, enthalpy and entropy of States 3 and 6 are calculated.
Condenser	Heater+ Heater	Heat duty of Condenser, temperature, enthalpy and entropy of States 9 and CW3 are calculated.
Evaporator	Heater+ Heater	Heat duty of Evaporator, temperature, enthalpy and entropy of State 11 and CoolWout are calculated.
Absorber	Mixer+ (Heater+ Heater)	Mass flow, enthalpy and entropy of State 12 are calculated. Heat duty of Absorber, temperature, enthalpy and entropy of CW2 are calculated.
Generator	HeatX+ Flash2	Heat duty of Generator, temperature, pressure, enthalpy and entropy of States 5 and 8 are calculated.

Please cite this article in press as: Wang, Y., et al., Optimal match between heat source and absorption refrigeration. Computers and Chemical Engineering (2016), http://dx.doi.org/10.1016/j.compchemeng.2016.11.003

Table 3
Physical properties of streams at heat source temperature 110 °C.

State(stream)	Temperature/°C	Pressure/Pa	Mass Flow /kg/s	Mass Fraction (LiBr)	h/kJ kg^{-1}	s/kJ kg^{-1} K^{-1}	h_0/kJ kg^{-1}	s_0/kJ kg^{-1} K^{-1}	E/kW
1	36.6	800	8	0.58	−9227.37	−3.78	−9250.23	−3.86	3.84
1A	36.6	800	8	0.58	−9227.38	−3.78	−9250.23	−3.86	3.84
2	36.6	9586	8	0.58	−9227.36	−3.78	−9250.23	−3.86	3.85
3	67.5	9586	8	0.58	−9167.08	−3.6	−9250.23	−3.86	45.62
4	89.5	9586	8	0.58	−9040.35	−3.24	−9250.23	−3.86	216.03
5	89.5	9586	7.74	0.6	−8897.86	−3.32	−9021.86	−3.69	95.33
6	57	9586	7.74	0.6	−8960.16	−3.5	−9021.86	−3.69	25.27
7	41.4	872	7.74	0.6	−8960.16	−3.49	−9021.86	−3.69	18.72
8	89.5	9586	0.26	0	−13312.06	−1.01	−15875.82	−9.06	42.29
9	45	9586	0.26	0	−15791.89	−8.78	−15875.82	−9.06	0.68
10	5	872	0.26	0	−15791.89	−8.74	−15875.82	−9.06	−2.37
11	5	872.6	0.26	0	−13474.08	−0.41	−15875.82	−9.06	−45.41
12	41.3	800	8	0.58	−9105.87	−3.39	−9250.23	−3.86	47.47
Coolwin	12	101325	28.55	0	−15930.2	−9.24	−15875.82	−9.06	33.77
Coolwout	7	101325	28.55	0	−15951.17	−9.32	−15875.82	−9.06	65.2
CW1	25	101325	22.5	0	−15875.46	−9.06	−15875.82	−9.06	0.53
CW2	35.3	101325	22.5	0	−15832.26	−8.91	−15875.82	−9.06	16.99
CW3	42.1	101325	22.5	0	−15803.79	−8.82	−15875.82	−9.06	45.16
HWin	110	202650	24	0	−15519.34	−8.01	−15875.82	−9.06	1091.28
HWout	100	202650	24	0	−15561.59	−8.12	−15875.82	−9.06	863.22

Table 4
Heat duty and exergy loss of each component at heat source temperature 110 °C.

Component	Heat duty/kW	Exergy loss/kW	Ratio in total exergy loss/%
Generator	1013.83	60.99	30.92
SHE	482.31	27.11	13.74
Condenser	640.39	41.56	21.07
Evaporator	598.56	10.18	5.16
Absorber	972.04	47.83	24.24
SolV	0	6.56	3.33
RefV	0	3.05	1.55
Pump	0.08	0.004	0.00
Sum		197.28	100

Table 5
Heat duty and exergy loss of each component at heat source temperature 120 °C.

Component	Heat duty/kW	Exergy loss/kW	Ratio in total exergy loss/%
Generator	1662.24	115.21	34.09
SHE	481.39	30.42	9.00
Condenser	1196.78	78.11	23.12
Evaporator	1100.3	18.94	5.60
Absorber	1566.06	85.49	25.30
SolV	0	4.12	1.22
RefV	0	5.68	1.68
Pump	0.08	0.004	0.00
Sum		337.97	100

Because the electricity consumed by the pump is negligible compared with heat input, COP can be expressed as

$$\mathrm{COP} = \frac{Cooling\ output}{heat\ input} \tag{1}$$

Exergy efficiency is

$$\eta_E = \frac{exergy\ of\ cooling\ output}{exergy\ of\ heat\ input} \tag{2}$$

Exergy of a stream, Ex, is obtained from Equation (3).

$$Ex = H - H_0 - T_0(S - S_0) \tag{3}$$

where H and S are the enthalpy and entropy of the stream, subscript 0 indicates the environmental state, and T_0 is the environmental temperature.

3. System performance at different heat source temperatures with a fixed evaporator temperature of 5 °C

In this section, we assess how the system performance changes with the heat source temperature at a fixed evaporator temperature of 5 °C.

When the heat source temperature is 110 °C, the physical properties of streams at each state can be simulated as shown in Table 3. From these properties, the exergy at each state can be calculated, as shown in the last column of Table 3. Furthermore, the heat duty and exergy loss of each component can be calculated as shown in Table 4 and Fig. 5.

At a certain evaporator temperature, if the heat source temperature is relatively low, which means the temperature difference between the heat source temperature and the saturated temperature of the solution is small, the generated refrigerant vapor flowrate will also be small. With increasing heat source temperature, the heat input increases so that the temperature difference between the heat source temperature and the saturated temperature of the solution becomes large, resulting in more refrigerant vapor being generated. The COP of the system will increase with increasing heat source temperature.

At a certain evaporator temperature, increasing the heat source temperature will increase the total exergy loss of the system because the difference between the input and output energy levels of the system becomes larger. In the generator, increasing the heat source temperature will generate more refrigerant vapor and increase the inlet and outlet temperatures of the working fluid so that the exergy loss increases due to the enlarged heat transfer temperature difference between the hot and cold streams. The heat duty and heat transfer temperature difference in the condenser will increase with increasing refrigerant vapor and generator temperature, resulting in an increase of exergy loss in the condenser. Although the temperatures of the hot and cold streams in the evaporator are unchanged, the exergy loss of the evaporator still increases due to the refrigerant vapor increase. In the absorber, the increased temperature of the rich solution to the absorber makes the heat transfer temperature difference between the hot and cold streams larger, and the increased refrigerant flowrate raises the heat duty, both of which enlarge the exergy loss. In the SHE, the temperature of the hot stream rises but that of the cold stream is almost unchanged because the solution flowrate from the generator decreases. The enlarged heat transfer temperature difference increases the exergy loss.

Table 5 gives the heat duty and exergy loss of each component at heat source temperature 120 °C. It can be seen by comparing Tables 4 and 5 that with the higher heat source temperature of 120 °C, exergy losses of almost all components increase, especially

Please cite this article in press as: Wang, Y., et al., Optimal match between heat source and absorption refrigeration. Computers and Chemical Engineering (2016), http://dx.doi.org/10.1016/j.compchemeng.2016.11.003

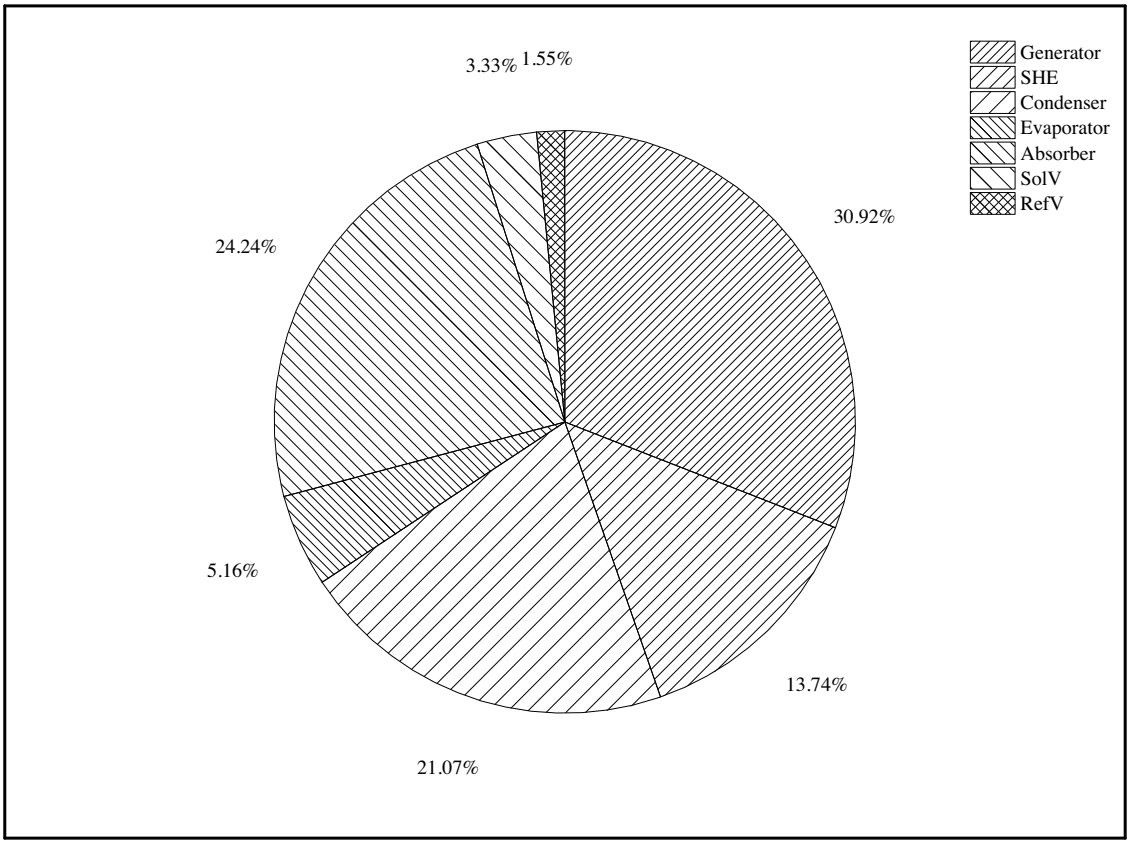

Fig. 5. Pie chart of exergy loss of each component at heat source temperature 110 °C.

those in the generator, condenser, evaporator and absorber. On the other hand, more refrigerant vapor is generated in the generator for more exergy input due to the higher temperature of the heat source, resulting in more exergy output. Because the extent of performance improvement is greater than the increase in the system exergy loss, the exergy efficiency increases by 14.4%.

However, since the increase of refrigeration load is less than that of heat input, as shown in Fig. 6, with increasing heat source temperature, the COP increases gradually, as shown in Fig. 7. When the heat source temperature increases over a certain extent, the increase in the system exergy loss will be greater than that of exergy output, as shown in Fig. 8. In this case, the exergy efficiency

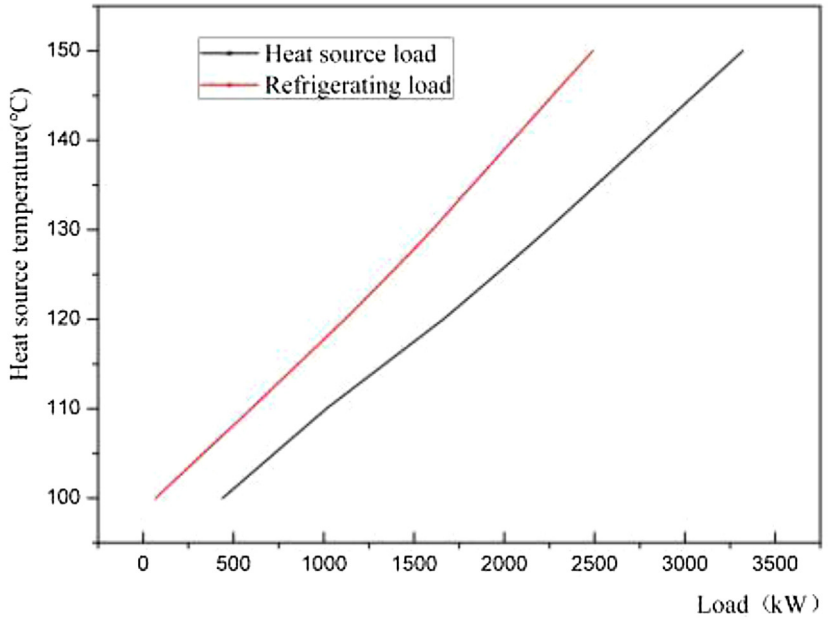

Fig. 6. Changes of heat input and refrigeration output with heat source temperature.

Please cite this article in press as: Wang, Y., et al., Optimal match between heat source and absorption refrigeration. Computers and Chemical Engineering (2016), http://dx.doi.org/10.1016/j.compchemeng.2016.11.003

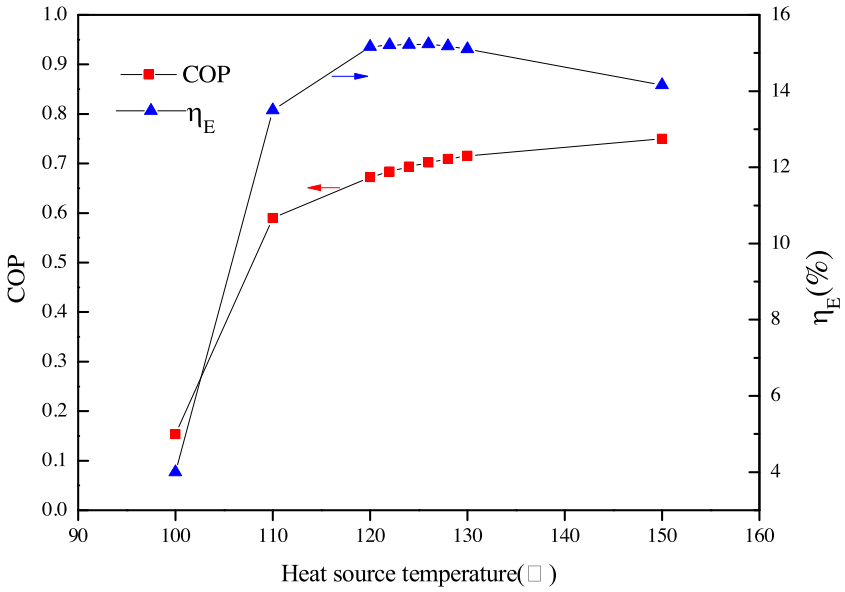

Fig. 7. System COP and exergy efficiency change with the heat source temperature at evaporator temperature 5 °C.

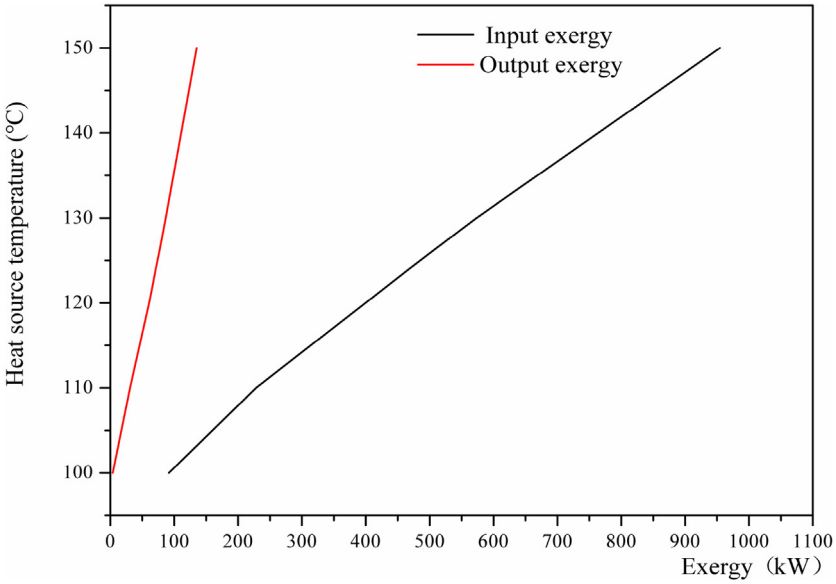

Fig. 8. Changes of exergy input and output with heat source temperature.

will decrease. Therefore, there is a maximum exergy efficiency, as shown in Fig. 7.

Table 6 shows the calculation results at different temperatures of the heat source at evaporator temperature 5 °C. Fig. 7 illustrates graphically how the system COP and exergy efficiency vary with the heat source temperature. The optimal temperature of the heat source is 126 °C at which the exergy efficiency reaches its maximum and the COP remains relatively high.

4. Optimal heat source temperatures at different evaporator temperatures

In the same way as described in section 3, the relationships of the system's COP and exergy efficiency with the heat source temperature at evaporator temperatures 8 °C, 11 °C and 15 °C are shown in Figs. 9, 10 and 11.

Fig. 12 illustrates the optimal heat source temperatures at the four evaporator temperatures studied here. It can be seen that when the evaporator temperature decreases, which indicates the quality of the cooling energy is higher, the heat source at higher temperature will be required, consequently the optimal heat source temperature will be higher. For cooling energy requirement at different temperature levels, there will be an optimal heat source to match it. Ensuring a proper selection of heat source for an absorption refrigeration cycle allows efficient use of the heat source and decreases degradation loss of the heat source.

5. Conclusion

Between heat source and refrigeration temperature level of an absorption refrigeration cycle, there is an optimal match with maximum exergy efficiency. In this paper, a single effect water–lithium bromide absorption refrigeration cycle is modeled and simulated using the process modeling software Aspen Plus. The optimal matches between heat source temperatures and refrigeration temperature levels of the absorption refrigeration cycle are determined.

Please cite this article in press as: Wang, Y., et al., Optimal match between heat source and absorption refrigeration. Computers and Chemical Engineering (2016), http://dx.doi.org/10.1016/j.compchemeng.2016.11.003

Table 6
Comparison of results at different heat source temperatures.

Heat source temperature/°C	Effective heat duty/kW	Refrigerant flowrate/kg/s	Cooling duty/kW	Exergy input/kW	Total exergy loss/kW	Exergy output/kW	COP	η_E/%
100	439.7	0.029	67.5	91.6	87.9	3.7	0.153	4.0
110	1013.8	0.260	598.6	228.1	197.3	30.8	0.590	13.5
120	1662.2	0.481	1117.3	399.6	339.0	60.6	0.672	15.16
122	1779.4	0.524	1216.4	433.4	367.5	65.9	0.683	15.21
124	1895.2	0.566	1314.1	467.6	396.5	71.1	0.693	15.21
126	2010.4	0.608	1410.9	502.4	425.9	76.5	0.702	15.23
128	2124.7	0.649	1506.6	537.7	456.1	81.6	0.709	15.18
130	2237.8	0.690	1601.0	573.3	486.8	86.6	0.715	15.1
150	3320.4	1.073	2489.7	954.4	819.3	135.1	0.750	14.2

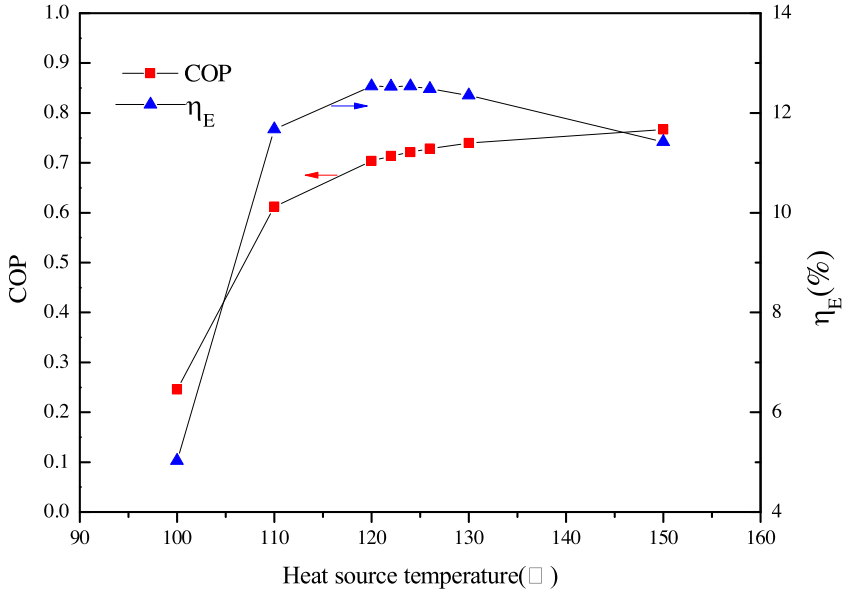

Fig. 9. System COP and exergy efficiency change with the heat source temperature at evaporator temperature 8 °C.

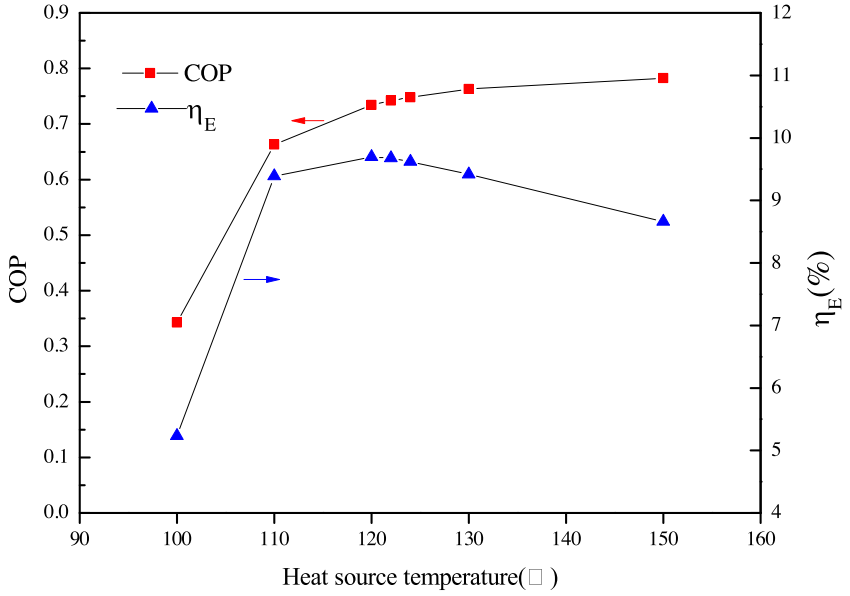

Fig. 10. System COP and exergy efficiency change with the heat source temperature at evaporator temperature 11 °C.

At a certain evaporator temperature of the absorption refrigeration cycle, the COP of the cycle increases with increasing heat source temperature because higher temperature generates more refrigerant vapor. Since the increase of refrigeration load is less than that of heat input, the COP of the cycle rises rapidly at first and then gently with increasing heat source temperature.

Please cite this article in press as: Wang, Y., et al., Optimal match between heat source and absorption refrigeration. Computers and Chemical Engineering (2016), http://dx.doi.org/10.1016/j.compchemeng.2016.11.003

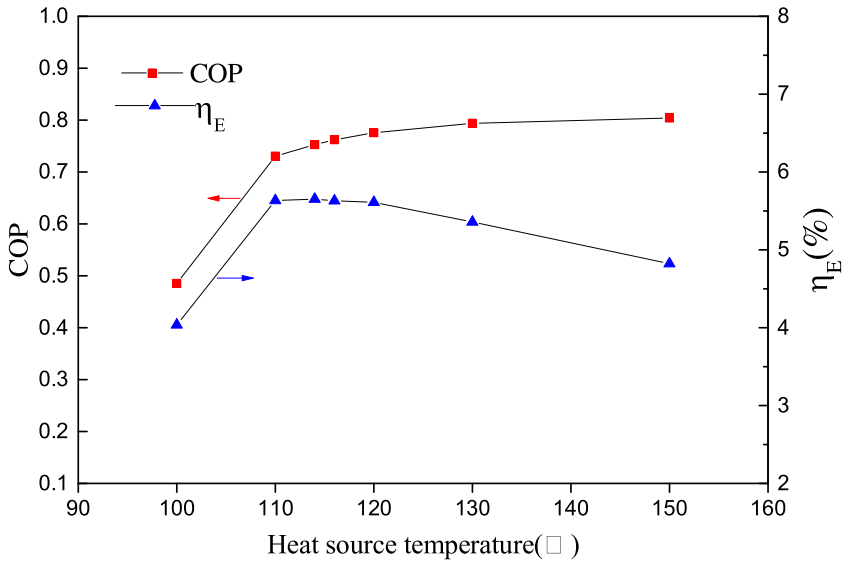

Fig. 11. System COP and exergy efficiency change with the heat source temperature at evaporator temperature 15 °C.

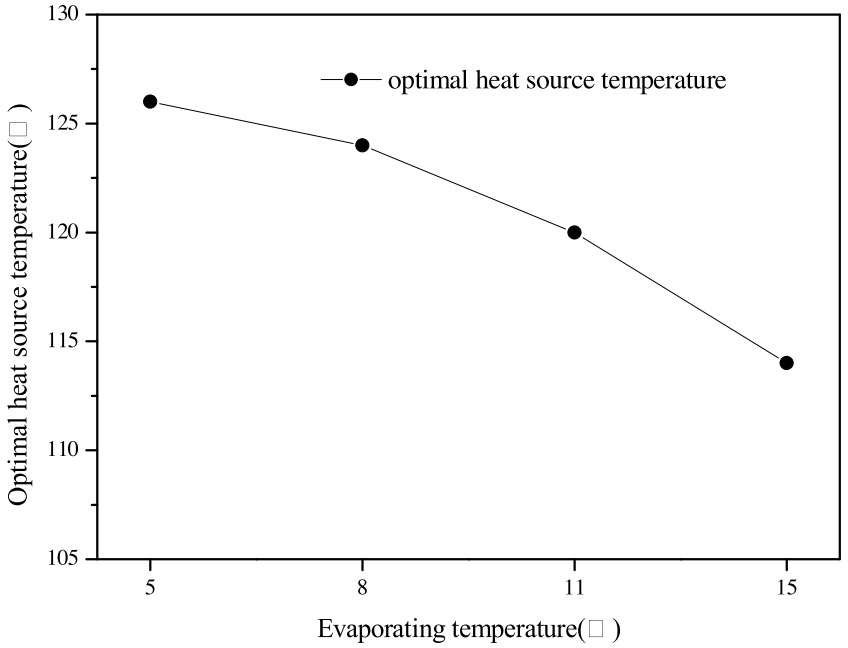

Fig. 12. Optimal heat source temperatures at different evaporator temperatures.

For the exergy efficiency of the cycle, at a certain evaporator temperature increasing the heat source temperature will result in an increase of the total exergy loss of the system because the difference between the input and output energy levels of the system becomes larger. With an increase in the heat source temperature, exergy input of the system rises to generate more refrigerant vapor which results in a corresponding increase in exergy output. If the extent of the system's performance improvement is greater than the increase of irreversibility, the exergy efficiency of the system will go up. Otherwise, the exergy efficiency will decrease. Therefore, to attain maximum exergy efficiency, there is an optimal heat source temperature for each refrigeration temperature level.

Ensuring a proper match between heat source and absorption refrigeration can lead to efficient use of the heat source and decrease degradation loss of the heat source.

Notation

CoolWin	Chilled water inlet
CoolWout	Chilled water outlet
COP	Coefficient of performance
CW	Cooling water
E	Exergy, kW
h	Specific enthalpy, kJ kg^{-1}
h_0	Specific enthalpy at benchmark state, kJ kg^{-1}
s	Specific entropy, kJ kg^{-1} K^{-1}
s_0	Specific entropy at benchmark state, kJ kg^{-1} K^{-1}
HWin	Hot water inlet
HWout	Hot water outlet
RefV	Throttle valve for refrigerant
SHE	Solution heat exchanger
SolV	Throttle valve for solution
η_E	Exergy efficiency

Please cite this article in press as: Wang, Y., et al., Optimal match between heat source and absorption refrigeration. Computers and Chemical Engineering (2016), http://dx.doi.org/10.1016/j.compchemeng.2016.11.003

Acknowledgement

Financial support from the National Natural Science Foundation of China (21576286) is gratefully acknowledged.

References

Anand, S., Gupta, A., Tyagi, S.K., 2013. Simulation studies of refrigeration cycles: a review. Renew. Sustain. Energy Rev. 17, 260.
Dai, Y., 2001. Water–Lithium Bromide Absorption Refrigeration Technology and Application. Mechanical Industry Press, Beijing.
Deng, J., Wang, R., Han, G., 2011. A review of thermally activated cooling technologies for combined cooling, heating and power systems. Prog. Energy Combust. Sci. 37, 172.
Ebrahimi, K., Jones, G.F., Fleischer, A.S., 2015. Thermo-economic analysis of steady state waste heat recovery in data centers using absorption refrigeration. Appl. Energy 139, 384.
Fernández-Seara, J., Vázquez, M., 2001. Study and control of the optimal generation temperature in NH_3–H_2O absorption refrigeration systems. Appl. Therm. Eng. 21, 343.
Gong, S., Boulama, K.G., 2014. Parametric study of an absorption refrigeration machine using advanced exergy analysis. Energy 76, 453.
Hammond, G.P., Norman, J.B., 2014. Heat recovery opportunities in UK industry. Appl. Energy 116, 387.
Karamangil, M.I., Coskun, S., Kaynakli, O., et al., 2010. A simulation study of performance evaluation of single-stage absorption refrigeration system using conventional working fluids and alternatives. Renew. Sustain. Energy Rev. 14, 1969.
Kaynakli, O., Kilic, M., 2007. Theoretical study on the effect of operating conditions on performance of absorption refrigeration system. Energy Convers. Manage. 48, 599.
Kaynakli, O., Saka, K., Kaynakli, F., 2015. Energy and exergy analysis of a double effect absorption refrigeration system based on different heat sources. Energy Convers. Manage. 106, 21.
Khan, M.M., Zaman, K., Irfan, D., Awan, U., Ali, G., Kyophilavong, P., Shahbaz, M., Naseem, I., 2016. Triangular relationship among energy consumption, air pollution and water resources in Pakistan. J. Clean. Prod. 112, 1375.
Kilic, M., Kaynakli, O., 2007. Second law-based thermodynamic analysis of water-lithium bromide absorption refrigeration system. Energy 32, 1505.
Law, R., Harvey, A., Reay, D., 2016. A knowledge-based system for low-grade waste heat recovery in the process industries. Appl. Therm. Eng. 94, 590.
Lian, H., Li, Y., Gu, C., 2011. An overview of domestic technologies for waste heat utilization. Energy Conservation Technology (Chinese) 29, 123.
Markides, C.N., 2013. The role of pumped and waste heat technologies in a high-efficiency sustainable energy future for the UK. Appl. Therm. Eng. 53, 197.
Mazzei, M.S., Mussati, M.C., Mussati, S.F., 2014. NLP model-based optimal design of LiBr-H_2O absorption refrigeration systems. Int. J. Refrig. 38, 58.
Reay, D.A., 1985. Heat recovery—an opportunity for process redesign or a case for retrofitting? J. Heat Recovery Syst. 5, 387.
Somers, C.M., 2009. Simulation of Absorption Cycles for Integration into Refining Processes. University of Maryland, Maryland.
Srikhirin, P., Aphornratana, S., Chungpaibulpatana, S., 2001. A review of absorption refrigeration technologies. Renew. Sustain. Energy Rev. 5, 343.

Please cite this article in press as: Wang, Y., et al., Optimal match between heat source and absorption refrigeration. Computers and Chemical Engineering (2016), http://dx.doi.org/10.1016/j.compchemeng.2016.11.003